

Millimeter-Wave Cavity-Backed Patch-Slot Dipole for Circularly Polarized Radiation

Xue Bai and Shi-Wei Qu

School of Electronic Engineering, University of Electronic Science & Technology
Chengdu, China
dyon.qu@gmail.com

Abstract—A novel millimeter-wave antenna for circularly polarized (CP) radiation is presented. The proposed antenna is composed of a patch dipole and a slot dipole, and it is realized by a plated through hole printed technique on a microwave substrate. Simulations show that the antenna can present a bandwidth from 55.8 to 65.3 GHz for a reflection coefficient (S_{11}) ≤ -10 dB as well as for an axial ratio (AR) ≤ 3 dB, and the 9.6 dBi average gain is achieved. This design yields good directional radiation patterns and low fabrication cost. Studies on several critical parameters are performed for practical designs.

Index Terms—Cavity-backed antennas, circular polarization, millimeter wave.

I. INTRODUCTION

Due to large capacity and high speed [1], the electromagnetic spectrum of 60-GHz band has drawn more and more attention. Meanwhile, circularly polarized (CP) radiation is very desirable for 60-GHz antennas because of its capabilities to reduce polarization mismatch and to suppress multipath interferences [2], for example they allow more flexible orientation of the transmitting and receiving antennas.

In microwave frequency bands, there are many ways to construct CP antennas, e.g., patches [3]-[6], crossed dipoles [7]-[10], and loop antennas [11]-[13]. However, it is difficult to construct these antennas in millimeter-wave (mm-wave) frequency bands, firstly because the very fine structures, especially the feeding network, cannot be realized. Moreover, a 90° power divider [8] or a balun [10] is necessary for the crossed dipoles, which obviously complicates the design.

On the other hand, on-chip CP antennas are popular due to the ease of system integration [14]. However, most of the on-chip antennas would suffer from low radiation gain. Other mm-wave off-chip CP antennas are typically expensive, owing to their tiny element size or preciseness in feed structures [15], [16] or high cost in micromachining process [17]. Although some low-cost designs have been proposed [18], the radiation patterns are unstable across the operating frequency band.

In this letter, a new implementation of cavity-backed patch-slot antenna on a substrate using plated through hole printed technology [19] is introduced for mm-wave CP applications. The CP radiation of the proposed antenna is realized by overlapping a patch dipole and a slot dipole to achieve two orthogonal electric field components and then by adjusting the connection between the patch and the slot to introduce 90° phase difference. The design yields good directional radiation patterns, low fabrication cost, and a 3-dB axial ratio (AR)

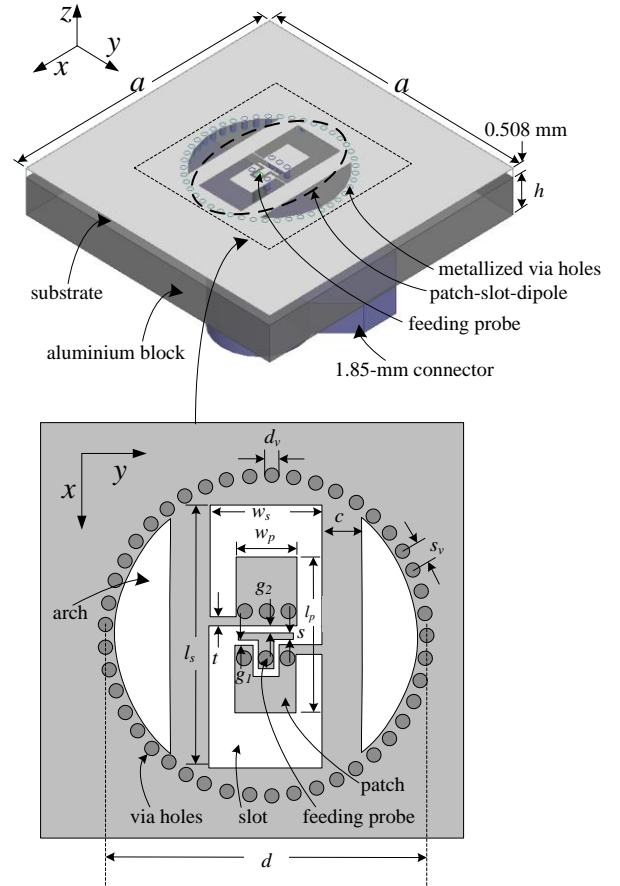


Fig. 1. Geometry of the proposed cavity backed patch-slot antenna for CP radiation. $a = 16$ ($3.2\lambda_0$), $d = 8$ ($1.6\lambda_0$), $h = 3.23$, $w_s = 2.8$ ($0.56\lambda_0$), $l_s = 6.5$ ($1.3\lambda_0$), $w_p = 1.5$ ($0.3\lambda_0$), $l_p = 3.9$ ($0.78\lambda_0$), $c = 1$, $t = 0.1$, $s = 0.15$, $g_1 = 0.05$, $g_2 = 0.25$, $d_v = 0.3$, $s_y = 0.56$ (in mm, λ_0 is the free-space wavelength at 60 GHz).

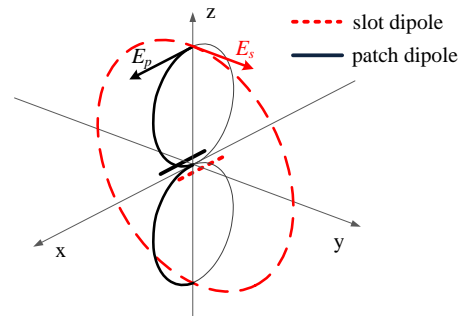


Fig. 2. Superposition of the electric fields of the patch and slot dipoles.

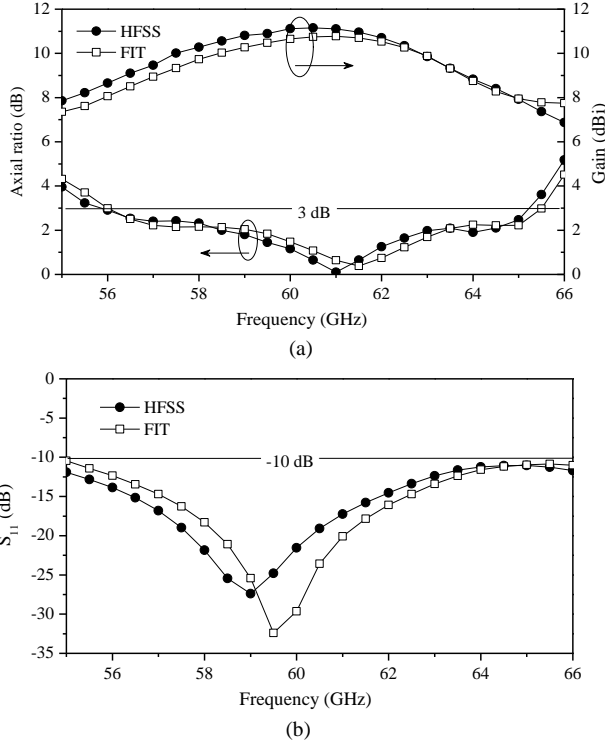


Fig. 3. Simulated results by FIT and HFSS, (a) simulated axial ratio and broadside gain, (b) simulated S_{11} .

bandwidth covering from 55.8 to 65.3 GHz, in which the reflection coefficient (S_{11}) is kept below -10 dB.

II. GEOMETRY

Fig. 1 shows geometry of the proposed cavity-backed patch-slot dipole antenna, and it consists of a patch-slot dipole, a cavity formed by metalized via holes, an aluminum block and a 1.85-mm connector for measurements. The patch dipole in [19] is introduced. Five metallic vias located at the center of the dipole are shorted to the ground plane. A special via hole acting as the feeding pin, is connected with a T-shaped coupled strip. The width and the length of the patch are w_p and l_p while those of the slot are w_s and l_s , respectively. To excite the slot dipole, two narrow strips with a width t connect the two broad edges of the slot to each arm of the patch dipole. Two arches are cut away beside the patch-slot dipole to make full advantage of the cavity. They are etched on a Rogers RT/duroid 5880(tm) substrate with an area of $a \times a$ (relative permittivity 2.2, thickness 0.508 mm, and $9\mu\text{m}$ cladding copper layer). The diameters of the cavity is d , and the height of the cavity shares the same value with the substrate, i.e., 0.508 mm.

Additionally, an aluminum block for supporting the antenna is mounted on the bottom of the substrate using conductive glue. A 50- Ω glass insulator with a probe (0.3 mm in diameter) is used to make sure accuracy of the feeding structure. Therefore, the height of the block should be designed according to the probe length of the glass insulator, i.e., $h = 3.23$ mm.

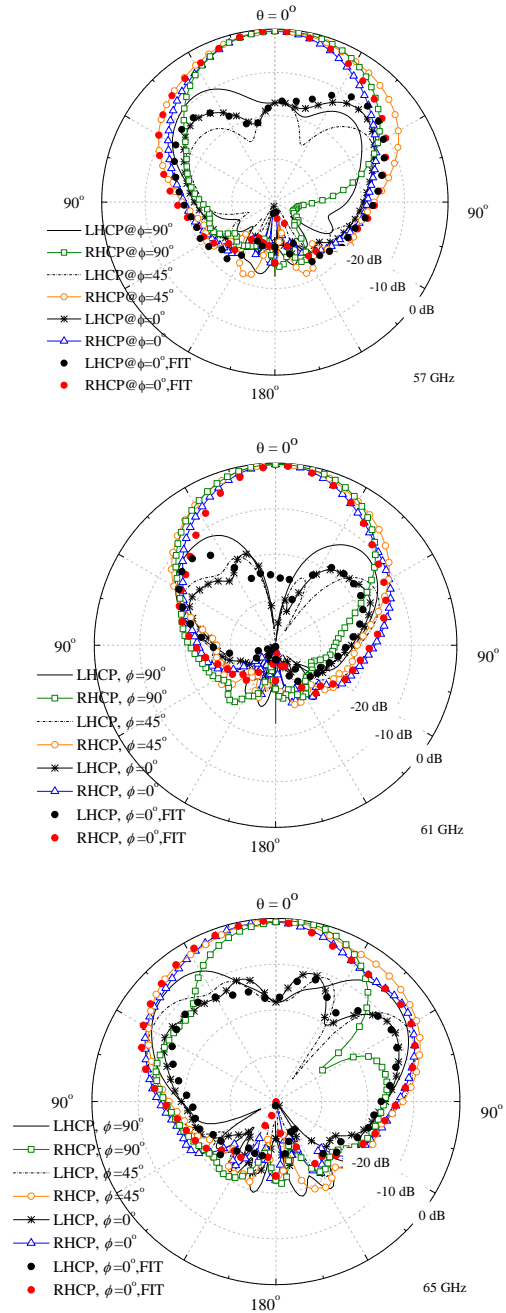


Fig. 4. Simulated radiation patterns by FIT and HFSS of the proposed antenna at 57, 61, and 65 GHz, respectively.

Fig. 2 depicts the design principle, in which a patch dipole and a slot dipole with complementary radiation characteristics are superposed. The radiation pattern of the patch dipole is in a shape of character “8” in the E plane (solid line) and of character “O” in the H plane, whereas the pattern of the slot dipole looks like “O” in the E plane and “8” in the H plane. Once the two dipoles are excited with proper amplitudes and phases, the CP radiation can be achieved in z-axis direction.

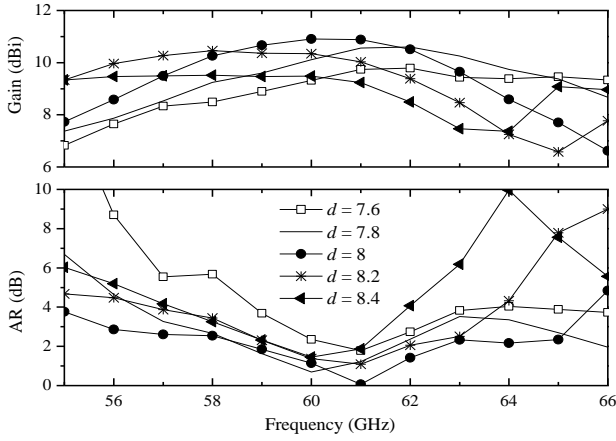


Fig. 5. Influence of d on broadside gain and axial ratio.

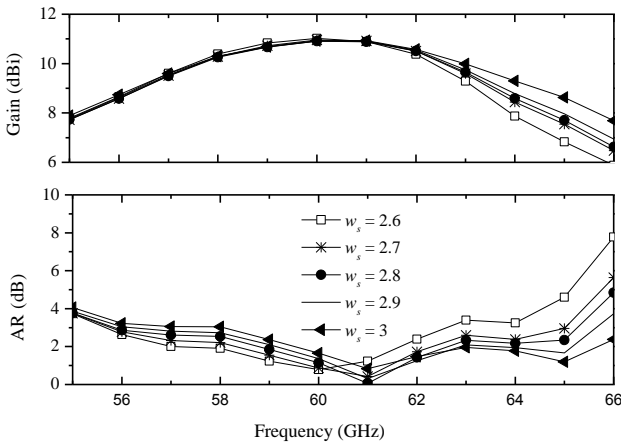


Fig. 6. Influence of w_s on broadside gain and axial ratio.

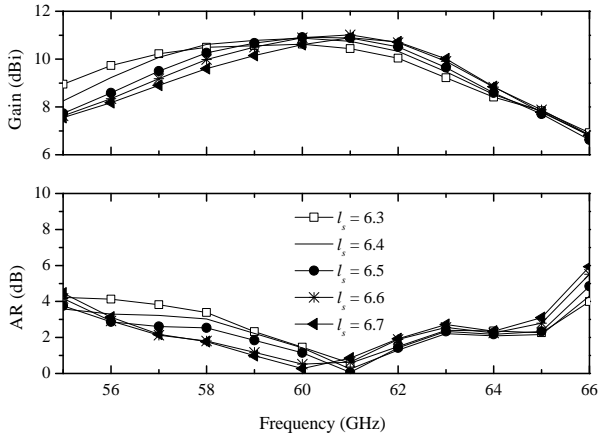


Fig. 7. Influence of l_s on broadside gain and axial ratio.

III. SIMULATED RESULTS

All simulations and optimizations are performed by the commercial software HFSSTM using the finite element method (FEM). The HFSS results are verified by the finite integration technique (FIT) additionally. The optimized parameters are shown in the caption of Fig. 1. The simulated broadside gains

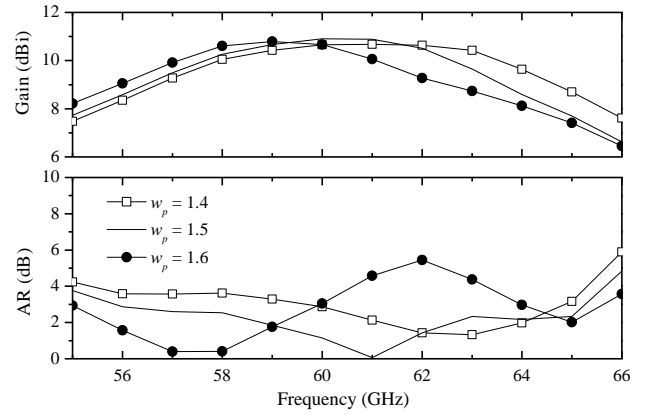


Fig. 8. Influence of w_p on broadside gain and axial ratio.

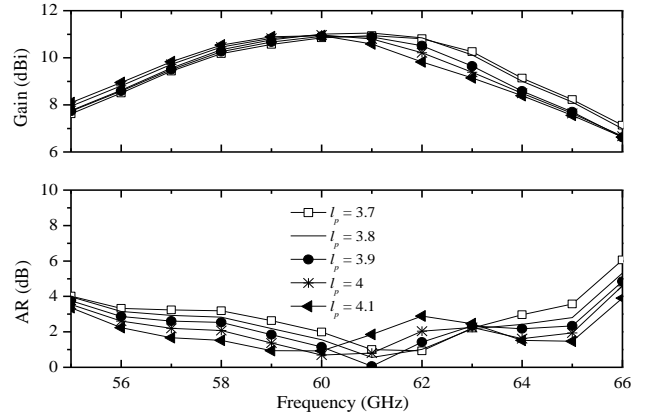


Fig. 9. Influence of l_p on broadside gain and axial ratio.

and ARs are shown in Fig. 3(a). The simulated frequency bandwidth for $AR \leq 3$ dB by FEM is 15.7%, covering from 55.8 to 65.3 GHz, in which the broadside gain is between 8 and 11.2 dBi with a maximum at 60.5 GHz. Comparatively, the FIT result is from 56.2 to 65.5 GHz, meanwhile the broadside gain is lower by around 0.5 dBi at frequencies below 61.5 GHz and matches the FEM results well at higher frequencies. Fig. 3(b) shows the simulated S_{11} of the proposed antenna, and the simulated S_{11} by FIT matches the FEM results reasonably. They are kept below -10 dB across the corresponding 3-dB AR bandwidth.

The simulated radiation patterns at 57, 61, and 65 GHz are shown in Fig. 4. The simulated patterns by FIT in $\phi = 0^\circ$ plane agree well with FEM results at these frequencies. It can be seen from the figure that the antenna presents symmetrical radiation patterns, small backward radiation (over -20 dB), without side lobes at lower frequencies. However, at higher frequencies, e.g., at 64 GHz, due to the increase of antenna electric size, the pattern in $\phi = 90^\circ$ plane is slightly distorted, but it still features a broadside radiation.

IV. PARAMETRIC STUDIES

To clearly show how each parameter controls the performance of the antenna, five critical parameters are

studied. When one parameter is studied, the others are kept to their optimized values in the caption of Fig. 1. Generally, the radiation performances, e.g., radiation patterns, broadside gain, axial ratio, and aperture efficiency are directly determined by the electric field distribution in the antenna aperture. Therefore, variations of the aperture dimensions will dramatically change its performances, as shown in Fig. 5. Too large or too small value of d not only significantly degrades the 3-dB AR bandwidth, but reduces the antenna gain. Note that according to our studies, a small variation of the parameters does not cause significant effects on the antenna impedance matching. Therefore, during the parametric studies, S_{11} are not given.

Fig. 6 shows the broadside gain and AR with different values of the width of the slot dipole w_s . At frequencies below 61 GHz, variation of w_s does not cause many effects on the broadside gain, but a larger w_s will worsen the CP performance. At frequencies above 61 GHz, a larger w_s is of benefit to both higher gain and lower AR.

The influence of the length of the slot dipole l_s on broadside gain and AR is shown in Fig. 7. As l_s is decreased, the maximum broadside gain is shifted downwards. Meanwhile, for a smaller l_s , it features a good AR at higher frequencies but a poor AR at lower frequencies.

The influence of the width of the patch dipole w_p on AR and gain is shown in Fig. 8. It can be seen that the CP performance is sensitive to the value of w_p , e.g., at 62 GHz as w_p is varied from 1.5 to 1.6 mm, the AR is significantly enlarged by 4 dB.

Fig. 9 shows the broadside gain and AR with different l_p , i.e., the length of the patch dipole. A larger l_p can obviously increase the 3-dB AR bandwidth, but at the middle frequencies it will worsen the CP performance. Meanwhile, at frequencies below 60 GHz the variation of l_p does not cause much effects on the broadside gain at lower frequencies, but at higher frequencies a smaller l_p is slightly of benefit to higher gain.

V. CONCLUSION

A novel CP cavity-backed antenna composed of a patch dipole and a slot dipole for millimeter wave applications is investigated. The vertical walls of the cavity are realized by a low-cost fabrication process of plated through hole printed technology on a microwave substrate. Its available 3-dB AR bandwidth is from 55.8 to 65.3 GHz, in which the S_{11} is kept below -10 dB, and the 9.6 dBi average gain has been achieved.

ACKNOWLEDGMENT

This work was partly supported by the Natural Science Foundation of China (NSFC) Projects under No. 61101036, and partly by the General Financial Grant from the China Postdoctoral Science Foundation under No. 2012M521682.

REFERENCES

- [1] T. Manabe, K. Sato, H. Masuzawa, K. Taira, K.-C. Huang, and D.J. Edwards, *Millimeter Wave Antennas for Gigabit Wireless Communications*. Chichester, U.K.: Wiley, 2008.
- [2] T. Ihara, Y. Kasashima, K. Yamaki, "Polarization dependence of multipath propagation and high-speed transmission characteristics of indoor millimeter-wave channel at 60 GHz," *IEEE Trans. Vehicular Technol.*, vol. 44, pp. 268–274, May 1995.
- [3] Nasimuddin, Z.-N. Chen, and X. Qing, "A compact circularly polarized cross-shaped slotted microstrip antenna," *IEEE Trans. Antennas Propag.*, vol. 60, pp. 1584–1588, Mar. 2012.
- [4] K. L. Chung, "A wideband circularly polarized H-shaped patch antenna," *IEEE Trans. Antennas Propag.* vol. 58, pp.3379–3383, Sep. 2010.
- [5] T.-N. Chang and J.-M. Lin, "Circular polarized ring-patch antenna," *IEEE Antennas Wirel. Propag. Lett.*, vol. 11, pp. 26–29, 2012.
- [6] K.-Y. Lam, K.-M. Luk, K.-F. Lee, H. Wong and K. B. Ng, "Small circular polarized u-slot wideband patch antenna," *IEEE Antennas Wirel. Propag. Lett.*, vol. 10, pp. 87–90, 2011.
- [7] J. Zhang, H.-C. Yang and D. Yang, "Design of a new high-gain circularly polarized antenna for inmarsat communication," *IEEE Antennas Wirel. Propag. Lett.*, vol. 11, pp.350–353, 2012.
- [8] K. M. Mak and M.-M. Luk, "A Circularly polarized antenna with wide axial ratio beamwidth," *IEEE Trans. Antennas Propag.* vol. 57, pp.3309–3312, Oct. 2009.
- [9] R. Li, D. C. Thompson, J. Papapolmerou, J. Lasker and M. M. Tentzeris "A circularly polarized short backfire antenna excited by an unbalance-fed cross aperture," *IEEE Trans. Antennas Propag.*, vol. 54, pp. 852–859, Mar. 2006.
- [10] S.-W. Qu, C. H. Chan, and Q. Xue, "Wideband and high-gain composite cavity-backed crossed triangular bowtie dipoles for circularly polarized radiation," *IEEE Trans. Antennas Propag.*, vol. 58, pp. 3157–3164, Oct. 2010.
- [11] Q. Yang, X. Zhang, N. Wang, X. Bai, J. Li, and X. Zhao, "Cavity-backed circularly polarized self-phased four-loop antenna for gain enhancement," *IEEE Trans. Antennas Propag.*, vol. 59, pp. 685–688, Feb. 2011.
- [12] S.-W. Qu, J.-L. Li, C. H. Chan, and Q. Xue, "Cavity-backed circularly polarized dual-loop antenna with wide tunable range," *IEEE Antennas Wirel. Propag. Lett.*, vol. 7, pp.761–763, 2008.
- [13] R. Li, B. Pan, J. Papapolmerou, J. Lasker and M. M. Tentzeris, "Development of a cavity-backed broadband circularly polarized slot/strip loop antenna with a simple feeding structure," *IEEE Trans. Antennas Propag.*, vol. 56, pp. 312–318, Feb. 2008.
- [14] X. Y. Bao, *et al.*, "60-GHz AMC-based circularly polarized on-chip antenna using standard 0.18- μ m CMOS technology," *IEEE Tran. Antennas Propagat.*, vol. 60, no. 5, pp. 2234–2242, May 2012.
- [15] C. Liu, Y.-X. Guo, X. Bao, and S.-Q. Xiao, "60-GHz LTCC integrated circularly polarized helical antenna array," *IEEE Tran. Antennas Propagat.*, vol. 60, no. 3, pp. 1329–1336, Mar. 2012.
- [16] Y. Li, Z. N. Chen, X. Qing, Z. Zhang, J Xu, and Z Feng, "Axial ratio bandwidth enhancement of 60-GHz substrate integrated waveguide-fed circularly polarized LTCC antenna array," *IEEE Tran. Antennas Propagat.*, vol. 60, no. 10, pp. 4169–4177, Oct. 2012.
- [17] M. Sun, Y.-O. Zhang, Y.-X. Guo, M. F. Karim, O. L. Chuen, and M. S. Leong, "Axial ratio bandwidth enhancement of 60-GHz substrate integrated waveguide-fed circularly polarized LTCC antenna array," *IEEE Tran. Antennas Propagat.*, vol. 59, no. 8, pp. 3083–3089, Aug. 2011.
- [18] A. D. Nestic and D. A. nestic, "Printed planar 8 \times 8 array antenna with circular polarization for millimeter-wave application," *IEEE Antennas Wirel. Propag. Lett.*, vol. 11, pp. 744–747, 2012.
- [19] K. B. Ng, H. Wong, K. K. So, C. H. Chan, and K. M. Luk, "60 GHz plated through hole printed magneto-electric dipole antenna," *IEEE Trans. Antennas Propag.*, vol. 60, pp. 3129–3137, Jul. 2012.